PROCEEDINGS OF SCIENCE

Electroweak probes in heavy-ion collisions with ATLAS

Iwona Grabowska-Bold[1,*]

AGH University of Science and Technology
Faculty of Physics and Applied Computer Science
Al. Mickiewicza 30, 30-059 Kraków, Poland

E-mail: Iwona.Grabowska@cern.ch

Electroweak bosons produced in lead-lead (Pb+Pb) collisions are an excellent tool to constrain initial-state effects which affect the rates of hard-scattering processes in nucleus-nucleus interactions. The production yields of massive electroweak bosons, observed via their leptonic decay channels, offer a high-precision test of the binary collision scaling expected in Pb+Pb and a way to quantify nuclear modifications of the parton distribution functions (PDFs).
The large samples of Pb+Pb data at $\sqrt{s_{\mathrm{NN}}}$ = 5.02 TeV collected by the ATLAS experiment in 2015, and the corresponding high-statistics *pp* data at the same collision energy used as a baseline, allow for a detailed experimental study of these phenomena and comparisons to predictions from a variety of theoretical calculations. This report presents the latest ATLAS results on electroweak boson production, including updated results on Z boson production and high-precision $W^{\pm}$ boson results in Pb+Pb collisions. Inclusive production of prompt photons in proton-lead (p+Pb) collisions at $\sqrt{s_{\mathrm{NN}}}$ = 8.16 TeV is also covered. Various predictions of nuclear modifications to PDFs are discussed.
A new measurement of light-by-light scattering in ultra-peripheral Pb+Pb collision data recorded in 2015 and 2018 at $\sqrt{s_{\mathrm{NN}}}$ = 5.02 TeV with an integrated luminosity of 2.2 nb^{-1} is also presented. Integrated and differential fiducial cross sections are measured. The invariant mass distribution of the diphoton system is used to extract limits on axion-like particles decaying to a two-photon system. This results in the most stringent limits to date over the diphoton mass range of 6-100 GeV.

HardProbes2020
1-6 June 2020
Austin, Texas

[1]On behalf of the ATLAS Collaboration
[*]Speaker

PoS(HardProbes2020)038

1. Electroweak bosons

Electroweak bosons ($W^{\pm}, Z, \gamma$) and leptons produced in $W^{\pm}$ or Z boson decays are not expected to interact substantially with the quark-gluon plasma (QGP) created in Pb+Pb collisions. This feature makes electroweak bosons excellent probes of the initial-state geometry of the heavy-ion collision. Moreover, p+Pb and proton-proton (pp) collisions are important references for the Pb+Pb system as they allow to disentangle initial- from final-state effects. In particular the p+Pb system is important to explore nuclear modifications to parton distributions functions (PDFs).

The ATLAS experiment [1] has measured inclusive prompt photon production in p+Pb collisions at $\sqrt{s_{\mathrm{NN}}}$ = 8.16 TeV with an integrated luminosity of 165 nb^{-1} [2]. The cross section and nuclear modification factor $R_{p\mathrm{Pb}}$ are measured as a function of the photon transverse energy, E_{T}^{γ}, from 20 to 550 GeV and in three nucleon-nucleon centre-of-mass pseudorapidity regions, η^{*}, spanning the range from -2.83 to 1.90. The cross section and $R_{p\mathrm{Pb}}$ values are compared with the results of a next-to-leading order (NLO) perturbative QCD (pQCD) calculation from JETPHOX [3], with (EPPS16, nCTEQ15) and without (CT14) nuclear modifications to the PDF. In Figure 1 the ratio of the $R_{p\mathrm{Pb}}$ values between forward and backward pseudorapidity is shown. This observable reduces the effect of common systematic uncertainties and thus allows to study the nuclear effects. The data is consistent with JETPHOX before incorporating nuclear effects, except possibly in the region $E_{\mathrm{T}}^{\gamma} < 55$ GeV, which is sensitive to the effects from gluon shadowing. At low E_{T}^{γ}, the data yields are systematically higher than the calculations which incorporate nuclear PDF effects, but approximately within their theoretical uncertainty.

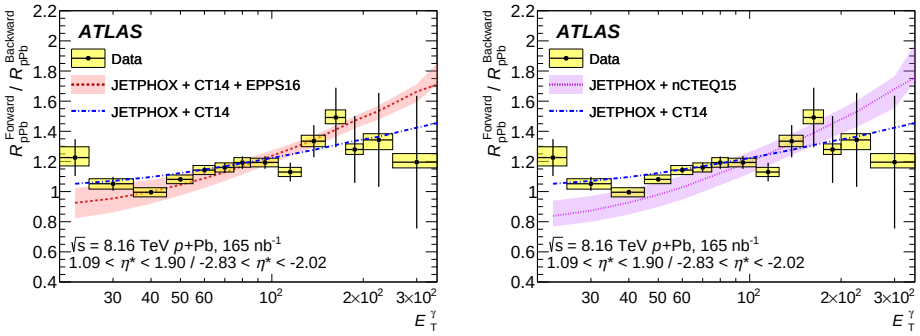

Figure 1: Ratio of the nuclear modification factor $R_{p\mathrm{Pb}}$ between forward and backward pseudorapidity for isolated, prompt photons as a function of E_{T}^{γ} [2]. The data are identical in each panel, and are compared to the expectations based on JETPHOX with (left) the EPPS16 nuclear PDF set or with (right) the nCTEQ15 nuclear PDF set. The yellow bands and vertical bars correspond to total systematic and statistical uncertainties in the data respectively. The red and purple bands correspond to the theoretical uncertainties in the calculations.

The $W^{\pm}$ and Z boson productions have been measured by the ATLAS experiment in Pb+Pb collisions at $\sqrt{s_{\mathrm{NN}}}$ = 5.02 TeV with an integrated luminosity of 0.49 nb^{-1} [4, 5]. Weak bosons are reconstructed using electron and muon decay channels. Production yields of $W^{\pm}$ bosons, normalised by the total number of minimum-bias events and the nuclear thickness function, are measured within a fiducial region defined by the detector acceptance and the kinematic requirements. Integrated fiducial cross sections for $W^{\pm}$ and Z boson productions obtained by ATLAS in pp collisions at $\sqrt{s}$ = 5.02 TeV are used for reference [6]. These normalised yields are measured separately for W^{+} and W^{-} bosons, and are presented as a function of the pseudorapidity of the charged lepton and of

the collision centrality. The results are compared with predictions based on NLO calculations with CT14 PDFs as well as with predictions obtained with the EPPS16 and nCTEQ15 nuclear PDFs.

The left panel of Figure 2 shows a comparison of combined production yields for W^+ bosons with theoretical predictions as a function of the charged-lepton pseudorapidity. The predictions are calculated using the MCFM code [7] at NLO accuracy in QCD. The calculations are performed using either the CT14 PDF set or EPPS16 and nCTEQ15 with modified PDFs. The predictions account for the isospin effect. All predictions provide a good description of the shapes of the measured $|\eta_\ell|$ distributions. The prediction based on the CT14 NLO PDF set differs by 2 – 3% in normalisation compared with the data, while the predictions based on nuclear PDFs underestimate the measured yields by 10 – 20%.

The right panel of Figure 2 shows the normalised Z boson yield compared between the combined measurement and the theoretical predictions calculated with the CT14, nCTEQ15 and EPPS16 NLO PDF sets. All calculations lie 1-3σ below the data in all rapidity intervals, integrated over event centrality. Calculations using nuclear PDF sets deviate from the data more strongly than calculations based only on the CT14 NLO PDF set.

It has been pointed out recently that the high precision of the ATLAS data on $W^\pm$ and Z bosons can be used to constrain the nucleon-nucleon inelastic cross section [8], which is important input to the Glauber modelling.

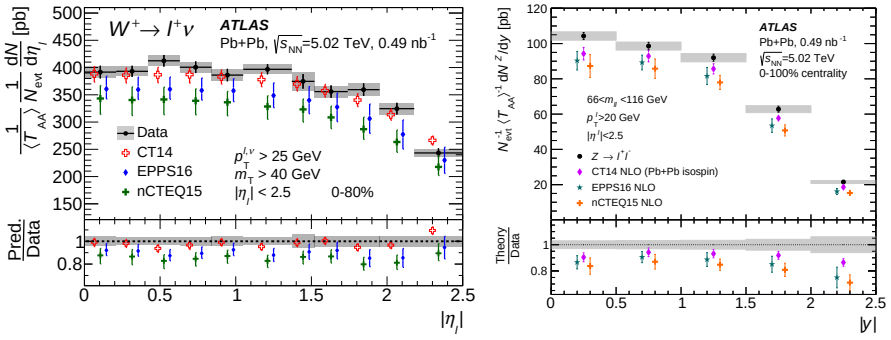

Figure 2: (Left) Differential production yields for W^+ bosons as a function of $|\eta_\ell|$ for the combined electron and muon channels [4]. The measured distributions are compared with theory predictions calculated with the CT14 NLO PDF set as well as with EPPS16 and nCTEQ15 nuclear PDF sets. (Right) Rapidity dependence of the normalised Z boson yields compared with theoretical predictions [5].

2. Light-by-light scattering and search for axion-like particles

The evidence of the light-by-light (LbyL) scattering process, $\gamma\gamma \to \gamma\gamma$, in ultra-peripheral Pb+Pb collisions at $\sqrt{s_{\rm NN}}$ = 5.02 TeV, followed by an observation, has been established by the ATLAS Collaboration [9, 10]. Those studies were based on 2015 and 2018 data sets analysed separately. In the new analysis of the LbyL process, the measurement is performed on the combined 2015+2018 data set [11] featuring an integrated luminosity of 2.2 nb^{-1}. As a result of improvements in the trigger efficiency and purity of the photon identification, a broader kinematic range in diphoton invariant mass (> 5 GeV) and single-photon transverse energy (> 2.5 GeV) is covered. This extension results in an increase of about 50% in expected signal yield in comparison with the previous measurements.

LbyL scattering candidates are selected in events with two photons produced exclusively, each with $E_{\mathrm{T}}^{\gamma} > 2.5$ GeV and pseudorapidity $|\eta_{\gamma}| < 2.4$, a diphoton invariant mass $m_{\gamma\gamma}$ above 5 GeV, and small diphoton transverse momentum and acoplanarity, $A_{\phi} = (1 - |\Delta\phi|/\pi)$, where $\Delta\phi$ stands for the difference in azimuthal angles of the two photon candidates. In order to suppress the $\gamma\gamma \to e^{+}e^{-}$ background, events are rejected if they have a charged-particle track with $p_{\mathrm{T}} > 100$ MeV, $|\eta| < 2.5$, and at least six hits in the pixel and microstrip detectors, including at least one pixel hit. To further suppress $\gamma\gamma \to e^{+}e^{-}$ events with poorly reconstructed charged-particle tracks, candidate events are required to have no "pixel tracks" matched to a photon candidate within $|\Delta\eta| < 0.5$. After applying all selection criteria including a requirement on $A_{\phi} < 0.01$, 97 candidate events are observed, where 45 signal and 27 background events are expected. After background subtraction and correction for detector inefficiency, an integrated fiducial cross section is measured as 120 ± 17 (stat.) ± 13 (syst.) ± 4 (lumi.) nb, which can be compared with the predicted values of 80 ± 8 nb from Ref. [12] and 78 ± 8 nb from SuperChic v3.0 Monte Carlo (MC) simulations [13]. The data-to-theory ratios are 1.50 ± 0.32 and 1.54 ± 0.32, respectively. The measurement is statistically limited. The systematic uncertainty is dominated by uncertainties in the trigger efficiency (5%) and photon reconstruction efficiency (4%).

Differential cross sections as a function of $m_{\gamma\gamma}$, diphoton absolute rapidity, average photon transverse momentum and diphoton $|\cos\theta^{*}|$, where θ^{*} is the $\gamma\gamma$ scattering angle in the $\gamma\gamma$ centre-of-mass frame, are unfolded to particle level in the fiducial phase space. The unfolded differential cross sections as a function of the invariant mass and absolute rapidity of the diphoton system are shown in Figure 3. They are compared with the predictions from SuperChic v3.0, which provide a fair description of the data, except for the overall normalisation differences.

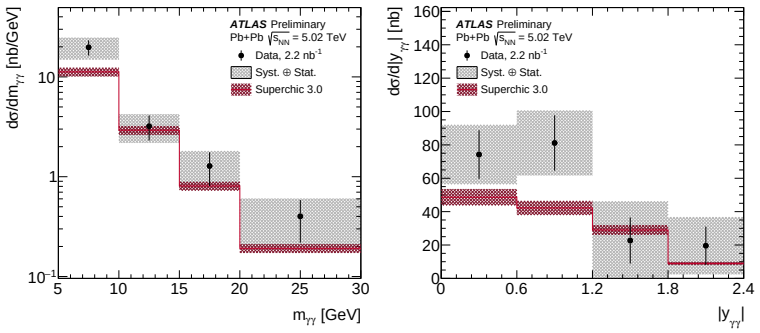

Figure 3: Measured differential cross sections of $\gamma\gamma \to \gamma\gamma$ production in Pb+Pb collisions at $\sqrt{s_{\mathrm{NN}}}$=5.02 TeV for (left) diphoton invariant mass and (right) diphoton absolute rapidity [11]. The measured cross-section values are shown as points with error bars giving the statistical uncertainty and grey bands indicating the size of the total uncertainty. The results are compared with the prediction from the SuperChic v3.0 MC generator (solid line) with bands denoting the theoretical uncertainty.

The measured diphoton invariant mass spectrum, as shown in the left panel of Figure 4, is used to search for axion-like particles (ALPs) via the $\gamma\gamma \to a \to \gamma\gamma$ reaction, where a denotes the ALP. The signal contribution is fitted using a maximum likelihood fit, which is then used to estimate the limit on the ALP signal strength at 95% confidence level (CL) using the asymptotic approximation. Those limits are transformed into limits on the ALP production cross section and

the ALP coupling to photons ($1/\Lambda_a$). Assuming a 100% ALP decay branching fraction to photons the derived constraints on the ALP coupling to photons are compared in the right panel of Figure 4 to those obtained from other experiments [14, 15]. The exclusion limits from this analysis are best so far over the mass range between 6 and 100 GeV.

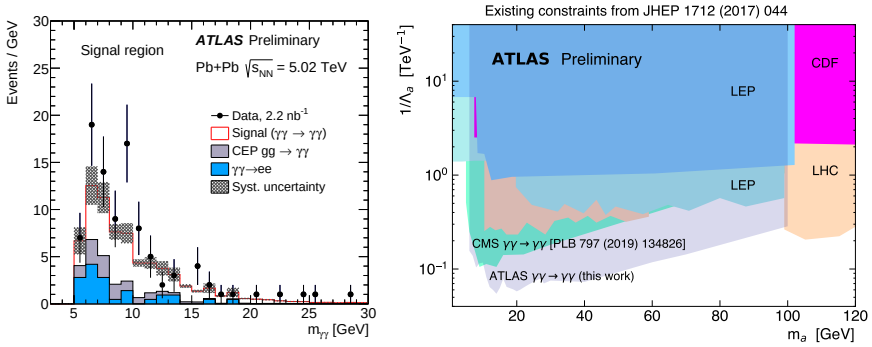

Figure 4: (Left) Diphoton invariant mass distribution for event candidates passing the LbyL selection [11]. Data (points) are compared to the sum of signal and background expectations (histograms). Systematic uncertainties on the signal and background processes, excluding that on the luminosity, are denoted as shaded bands. (Right) Compilation of exclusion limits at 95% CL in the ALP-photon coupling ($1/\Lambda_a$) versus ALP mass (m_a) plane obtained by different experiments. The existing limits, derived from Refs. [14, 15] are compared to the limits extracted from this measurement. The exclusion limits denoted as "LHC" are based on *pp* collision data from ATLAS and CMS.

Acknowledgements

This work was partly supported by the AGH UST statutory task No. 11.11.220.01/4 within subsidy of the Ministry of Science and Higher Education, by the National Science Centre of Poland under grant number UMO-2016/23/B/ST2/01409, and by PL-GRID infrastructure.

References

[1] ATLAS Collaboration, JINST 3 (2008) S08003, doi:10.1088/1748-0221/3/08/S08003.

[2] ATLAS Collaboration, Phys. Lett. B 796 (2019) 230, doi:10.1016/j.physletb.2019.07.031.

[3] P. Aurenche, M. Fontannaz, J.-P. Guillet, E. Pilon and M. Werlen, Phys. Rev. D 73 (2006) 094007, doi:10.1103/PhysRevD.73.094007.

[4] ATLAS Collaboration, Eur. Phys. J. C 79 (2019) 935, doi:10.1140/epjc/s10052-019-7439-3.

[5] ATLAS Collaboration, Phys. Lett. B 802 (2020) 135262, doi:10.1016/j.physletb.2020.135262.

[6] ATLAS Collaboration, Eur. Phys. J. C 79 (2019) 128, doi:10.1140/epjc/s10052-019-6622-x.

[7] J. M. Campbell, R. K. Ellis and W. T. Giele, Eur. Phys. J. C 75 (2015) 246, doi:10.1140/epjc/s10052-015-3461-2.

[8] K. J. Eskola, I. Helenius, M. Kuha, H. Paukkunen, doi:arXiv:2003.11856.

[9] ATLAS Collaboration, Nature Phys. 13 (2017) 9, doi:10.1038/nphys4208.

[10] ATLAS Collaboration, Phys. Rev. Lett. 123 (2019) 052001, doi:10.1103/PhysRevLett.123.052001.

[11] ATLAS Collaboration, ATLAS-CONF-2020-010, http://cdsweb.cern.ch/record/2719516.

[12] M. Klusek-Gawenda, P. Lebiedowicz and A. Szczurek, Phys. Rev. C 93 (2016) 044907, doi:10.1103/PhysRevC.93.044907.

[13] L. A. Harland-Lang, V. A. Khoze and M. G. Ryskin, Eur. Phys. J. C 79 (2019) 39, doi:10.1140/epjc/s10052-018-6530-5.

[14] CMS Collaboration, Phys. Lett. B 797 (2019) 134826, doi:10.1016/j.physletb.2019.134826.

[15] M. Bauer, M. Neubert and A. Thamm, JHEP 12 (2017) 044, doi:10.1007/JHEP12(2017)044.